Bioresource Technology 112 (2012) 151–155

Contents lists available at SciVerse ScienceDirect

Bioresource Technology

journal homepage: www.elsevier.com/locate/biortech

Kinetic study of acid-catalyzed cellulose hydrolysis in 1-butyl-3-methylimidazolium chloride

Zehui Zhang [a,d,1], Weiqi Wang [b,1], Xiangyue Liu [b], Qian Wang [a,c], Weixue Li [b], Haibo Xie [a,c,*], Zongbao K. Zhao [a,c,*]

[a] Division of Biotechnology, Dalian Institute of Chemical Physics, CAS, 457 Zhongshan Road, Dalian 116023, China
[b] The State Key Laboratory of Catalysis, Dalian Institute of Chemical Physics, CAS, 457 Zhongshan Road, Dalian 116023, China
[c] Dalian National Laboratory for Clean Energy, Dalian 116023, China
[d] Key Laboratory of Catalysis and Materials Sciences of the State Ethnic Affairs Commission & Ministry of Education, College of Chemistry and Material Science, South-Central University for Nationalities, Wuhan 430074, China

ARTICLE INFO

Article history:
Received 6 December 2011
Received in revised form 11 February 2012
Accepted 15 February 2012
Available online 22 February 2012

Keywords:
Cellulose
Hydrolysis
Ionic liquids
Kinetic equations

ABSTRACT

In this paper, the kinetics of acid-catalyzed cellulose hydrolysis in ionic liquids (ILs) was investigated by using 1-butyl-3-methylimidazolium chloride ([Bmim]Cl) as the model IL. General kinetic equations for the formation of glucose as well as cellooligomers were constructed at a molecular level, assuming that cellulose is fully dissolved to form a homogenous solution and that the scission of the glycosidic bond occurs randomly within the cellulose chain. Experimental data were well fitted according to these equations. Variations of kinetic parameters in the presence of different water content indicated that water behaved also as a base to decrease the acidity of the reaction medium. More importantly, it offered a profile of the evolution of cellooligomers. These results provided insights into the detailed mechanisms of cellulose hydrolysis in a non-aqueous, homogenous environment and should be valuable for developing strategies to depolymerize lignocellulosic biomass.

1. Introduction

Biomass represents a promising carbon-based alternative as an energy source and a sustainable chemical feedstock (Sheldon, 2011; Chheda et al., 2007). To facilitate a more efficient biotransformation, monomeric sugars have to be prepared by hydrolysis of (hemi)cellulose presented in biomass. Thus, the hydrolysis process is intensively studied to improve the efficiency and economics (Blanch et al., 2011). Recently, it was found that ionic liquids (ILs) can dissolve cellulose (Swatloski et al., 2002) as well as raw lignocellulosic materials (Kilpelainen et al., 2007). It was demonstrated that cellulose could be depolymerized in ILs in the presence of a catalytic amount of mineral acids to afford glucose and total reducing sugars in good yields (Li and Zhao, 2007). Later, a number of similar studies have been carried out using solid acids (Rinaldi et al., 2008, 2010; Zhang and Zhao, 2009) as well as mineral acids (Rinaldi et al., 2010; Vanoye et al., 2009; Li et al., 2008; Binder and Raines, 2010) as the catalysts.

Kinetics of acid-catalyzed cellulose hydrolysis under an aqueous environment has been studied (Saeman, 1945; Fagan et al., 1971; Thompson and Grethlein, 1979). A two consecutive first-order reaction model was proposed for the dilute-acid catalyzed cellulose hydrolysis, and experimental data were well fit into the model (Saeman, 1945). Because cellulose was not solubilized and physio-chemical properties of cellulose varied substantially during the course of the experiment, it turned out challenging to reach an insightful view for the hydrolysis process. Thus, kinetic studies based on this early model led to different kinetic parameters (Fagan et al., 1971; Thompson and Grethlein, 1979). Moreover, it was difficult to link those kinetic parameters to detailed reaction mechanism.

Homogenous cellulose hydrolysis in ILs is expected to have distinct kinetics. One of the most important features is to accumulate sugar oligomers over time. The production of oligosaccharides has already been pursued (Rinaldi et al., 2008; vom Stein et al., 2010). Interestingly, the formation of cellobiose and other oligomers can be advantageous for downstream biotransformations, because these water-soluble products can provide an approach to circumvent the notorious "glucose effect" which significantly reduces the efficiency of microbial transformations (Ha et al., 2011). Recently, a kinetic equation for glucose formation from cellulose in ILs was developed based on a first-order random chain scission

* Corresponding authors at: Division of Biotechnology, Dalian Institute of Chemical Physics, CAS, 457 Zhongshan Road, Dalian 116023, China. Tel.: +86 411 84379066; fax: +86 411 84379211.
E-mail addresses: hbxie@dicp.ac.cn (H. Xie), zhaozb@dicp.ac.cn (Z.K. Zhao).
[1] These authors contributed equally to this manuscript.

0960-8524/$ - see front matter © 2012 Elsevier Ltd. All rights reserved.
doi:10.1016/j.biortech.2012.02.071

followed by a first-order glucose degradation (Vanoye et al., 2009). However, the formation of cellooligomers, for example, cellobiose, has not been addressed. In another study, the reaction profile of cellulose hydrolysis in ILs catalyzed by hydrogen chloride was described, but kinetic equations were not proposed (Rinaldi et al., 2010). In this context, it remains interesting to look into the kinetic details of homogeneous cellulose hydrolysis.

The present work reports the kinetics of acid-catalyzed cellulose hydrolysis in ILs. General kinetic equations for the estimation of glucose as well as cellooligomers were constructed at a molecular level, and experimental data were fit well according to these equations. In particular, some parameters of the hydrolysis process were identified, and the profiles of cellooligomers evolution were also obtained. These results provided insights into the detailed mechanisms of homogeneous cellulose hydrolysis in a non-aqueous environment and should be valuable for developing strategies to depolymerize cellulose and lignocellulosic biomass.

2. Experimental

2.1. Materials

Spruce cellulose (Cat. No. 22182) was purchased from Sigma (St. Louis, USA), and was dried under vacuum at 100 °C for 24 h before use. Ionic liquid 1-butyl-3-methylimidazolium chloride ([Bmim]Cl) was supplied by Lanzhou Greenchem ILS, LICP, CAS (Lanzhou, China). Sulfuric acid (98 wt.%) was of analytical grade. Ultrapure water was generated by Milli-Q system (Bedford, USA).

2.2. Typical procedure for cellulose hydrolysis

A mixture of cellulose (0.24 g, 1.5 mmol AGU) in [Bmim]Cl (4.0 g) was heated with stirring at 94 °C in a 10-mL round bottomed flask with a lip until a clear solution was formed. To this solution was added a set amount of ultrapure H_2O and 56 mg 98 wt.% H_2SO_4 (0.56 mmol). Samples were withdrawn, weighed (usually less than ca. 50 mg), quenched with water, and the aqueous solution was centrifuged at 10,000 rpm for 5 min, then diluted with deionized water to appropriate concentrations for ion chromatography analysis.

2.3. Determination of glucose and cellobiose

Glucose and cellobiose were analyzed by using the ion chromatography ICS-2500 system (Dionex, USA) equipped with a GP50 gradient pump, an ED50A integrated amperometry detector, a CarboPac PA10 guard column (4 mm × 50 mm), a high capacity CarboPac PA20 analytical column (3 mm × 150 mm), a 25 μL sample loop (Zhang et al., 2011). Samples (20 μL) were injected and eluted with 30 mmol/L NaOH at a rate of 0.5 mL/min. Glucose and cellobiose standards were used to generate standard curves for quantification purpose.

3. Results and discussion

3.1. Developing kinetic equations for cellulose hydrolysis

Cellulose, the major component of lignocellulosic materials, is composed of β-(1 → 4)-linked anhydroglucose units (AGU). However, due to the extensive network of inter- and intra-molecule hydrogen bonds and van der Waals interactions, cellulose is insoluble in most conventional solvents, leading to notoriously recalcitrant to processing (Nishiyama et al., 2003). Yet, progresses have been continuously made. For example, the depolymerization of cellulose and lignocelluloses was reported by using cyanuric chloride to increase glucose yield (Jiang et al., 2012). Autoclave parr reactor system was also developed for the hydrolysis of municipal bio-wastes catalyzed by dilute phosphoric acid to obtain xylose and glucose in 100% and 30% yield, respectively (Orozco et al., 2011). Acid-catalyzed hydrolysis of cellulose could be realized efficiently in ILs, likely because the reaction took place in a homogenous solution (Li and Zhao, 2007). Thus, individual cellulose molecules are expected fully accessible for hydrolysis. Moreover, acid-catalyzed scission of the glycosidic bond should occur randomly within the cellulose chain, because there is no driving force for regio-selectivity. Apparently, the ILs system distinguishes from conventional systems where hydrolysis reaction takes place at the cellulose matrix surface.

To simplify the discussion of kinetic equations, O_n is used to represent a cellulose molecule with a DP (degree of polymerization) value of n, where the symbol "O" represents the glucose unit. Thus, a hydrolytic step can be written as $O_n \rightarrow O_m + O_{n-m}$ ($m < n$). At least three chemical steps are involved to facilitate a glycosidic bond cleavage in the presence of an acid (Rinaldi and Schüth, 2009). The first step for the protonation of the glycosidic oxygen is assumed a fast equilibrium reaction with the equilibrium constant K_1 (Supplementary Fig. 1). Then the protonated glycosidic bond cleaves to form a six-membered cyclic cation with the rate constant k_2. This step is slow and assumed rate-limiting. Finally, a water molecule attacks the cyclic cation leading to the formation of the reducing end and the release of a proton. This step is a fast one.

When considering a system with the cellulose molecule O_n at an initial concentration of C_0, an illustrative scheme can be written as,

	1	-	2	-	3	-	⋯	n-1	-	n
1	O	$b_{1,1}$	O	$b_{2,1}$	O	$b_{3,1}$	⋯	O	$b_{n-1,1}$	O
2	O	$b_{1,2}$	O	$b_{2,2}$	O	$b_{3,2}$	⋯	O	$b_{n-1,2}$	O
3	O	$b_{1,3}$	O	$b_{2,3}$	O	$b_{3,3}$	⋯	O	$b_{n-1,3}$	O
⋮	⋮									⋮
C_0	O	b_{1,C_0}	O	b_{2,C_0}	O	b_{3,C_0}	⋯	O	b_{n-1,C_0}	O

In the above scheme, adjacent O in the same row is linked by "b", the symbol for the glycosidic bond. The linkage between the ith O and the $(i+1)$th O in the jth row is indicated by $b_{i,j}$ ($i < n$, $j < C_0$). No linkage is allowed between "O" from different rows. It is obvious that cellulose hydrolysis is essentially to break the glycosidic bonds, and thus, depending on the concentration of "b", $[b]$. When a strong acid, such as sulfuric acid, is used, a complete dissociation is expected to give a free proton concentration (C_H). It should be pointed out that the presence of the hydrolytic products O_m should not change the probability of the first step and the rate of the second rate of cellulose hydrolysis (r_h) can be written as Eq. (1), according to the reaction mechanism

$$r_h = K_1 k_2 C_H [b] \quad (1)$$

As shown in Eq. (1), the overall rate constant (k_h) is the product of K_1 with k_2. Therefore, the reaction rate can also be expressed as Eq. (2). When the reaction is performed in the presence of a known amount of acid, the term C_H is a constant. Thus, the hydrolysis reaction is first-ordered with respect to $[b]$ under the specific conditions

$$r_h = k_h C_H [b] \quad (2)$$

The bond concentration of $[b]$ can be obtained from Eq. (2) by separation of variables and then integral to give Eq. (3)

$$[b] = e^{\ln[C_0 \times (n-1)] - k_h C_H t} \quad (3)$$

An adjacency matrix $B[i,j]$ based on the element "b" is constructed, which is derived from the above scheme. The value of each element $b_{i,j}$ is either 0 or 1, where 1 indicates that the glycosidic bond between the ith O and the $(i+1)$th O in the jth row remains intact, while 0 indicates the glycosidic bond is broken.

	b_0	b_1	b_2	⋯	b_{n-1}	b_n
1	0	$b_{1,1}$	$b_{2,1}$	⋯	$b_{n-1,1}$	0
2	0	$b_{1,2}$	$b_{2,2}$	⋯	$b_{n-1,2}$	0
3	0	$b_{1,3}$	$b_{2,3}$	⋯	$b_{n-1,3}$	0
⋮	⋮	⋮			⋮	⋮
C_0	0	b_{1,C_0}	b_{2,C_0}	⋯	b_{n-1,C_0}	0

In order to understand the reaction more easily, two columns, b_0 and b_n, are added into the matrix $B[i,j]$, and the values of both b_0 and b_n equal to 0, indicating that no additional "O" is attached at either end of the cellulose chain. As the glycosidic bonds are protonated randomly, the glycosidic bonds share the same probability to be cleaved in the hydrolysis process. Therefore, the probability that element $b_{i,j}$ in the adjacency matrix to be 1 can be expressed as shown in Eq. (4)

$$P_{(b_{i,j}=1)} = \frac{[b]}{(n-1)\times C_0} = \frac{e^{\ln[(n-1)\times C_0]-k_h C_H t}}{(n-1)\times C_0} \tag{4}$$

Accordingly, the probability that element $b_{i,j}$ in the adjacency matrix to be 0 can be expressed as shown in Eq. (5)

$$P_{(b_{i,j}=0)} = 1 - \frac{[b]}{(n-1)\times C_0} = 1 - \frac{e^{\ln[(n-1)\times C_0]-k_h C_H t}}{(n-1)\times C_0} \tag{5}$$

Therefore, the concentrations of the monomer O_1 and oligomers O_m has a direct relationship with the element $b_{i,j}$ in the adjacency matrix $B[i,j]$. To obtain the monomer O_1, the values of both $b_{i-1,j}$ and $b_{i,j}$ should equal to 0. Thus, $[O_1]$ can be obtained according to Eq. (6)

$$\begin{aligned}[O_1] &= \sum_{j=1}^{C_0}\left\{P_{(b_{1,j}=0)} + \sum_{i=1}^{n-2}[P_{(b_{i,j}=0)}\times P_{(b_{i+1,j}=0)}] + P_{(b_{n-1,j}=0)}\right\} \\ &= C_0\times\left\{2\times P_{(b_{i,j}=0)} + (n-2)\times[P_{(b_{i,j}=0)}]^2\right\}\end{aligned} \tag{6}$$

Likewise, Eq. (6) can be extended to fit other cellooligomers with a DP of m, in which case values of elements $b_{i-1}j$, b_ij, $b_{i+1}j\ldots b_{i+m-1,j}$ and $b_{i+m}j$ should be $0,1,1,\ldots,1$ and 0, respectively. Consequently, $[O_m]$ can be expressed as shown in Eq. (7)

$$\begin{aligned}[O_m] &= \sum_{j=1}^{C_0}\left\{2\times\left(P_{(b_{i,j}=1)}\right)^{m-1}\times P_{(b_{i,j}=0)} + \sum_{i=1}^{n-m-1}\left[\left(P_{(b_{i,j}=0)}\right)^2\times\left(P_{(b_{i+1,j}=1)}\right)^{m-1}\right]\right\} \\ &= C_0\times\left\{2\times\left(P_{(b_{i,j}=1)}\right)^{m-1}\times P_{(b_{i,j}=0)} + (n-m-1)\times\left(P_{(b_{i,j}=0)}\right)^2\times\left(P_{(b_{i+1,j}=1)}\right)^{m-1}\right\}\end{aligned} \tag{7}$$

Upon incorporation of Eqs. (4) and (5) into the Eqs. (6) and (7), respectively, Eqs. (8) and (9) are obtained

$$[O_1] = C_0\times\left[2\times\left(1-\frac{e^{\ln[(n-1)\times C_0]-k_h C_H t}}{(n-1)\times C_0}\right) + (n-2)\times\left(1-\frac{e^{\ln[(n-1)\times C_0]-k_h C_H t}}{(n-1)\times C_0}\right)^2\right] \tag{8}$$

$$\begin{aligned}[O_m] = C_0\times&\left(\frac{e^{\ln[(n-1)\times C_0]-k_h C_H t}}{(n-1)\times C_0}\right)^{m-1} \\ &\times\left[2\times\left(1-\frac{e^{\ln[(n-1)\times C_0]-k_h C_H t}}{(n-1)\times C_0}\right) + (n-m-1)\times\left(1-\frac{e^{\ln[(n-1)\times C_0]-k_h C_H t}}{(n-1)\times C_0}\right)^2\right]\end{aligned} \tag{9}$$

To take the O_1 degradation reaction into consideration, these equations have to be modified further. It is known that the degradation of glucose is first-ordered when the concentration of free proton (C_H) is held constant (vom Stein et al., 2010). The rate constant for the O_1 degradation reaction is assigned as k_0. Therefore, an actual concentration for the monomer O_1, namely $[O_{1d}]$ can be expressed as shown in Eq. (10)

$$dO_{1d} = dO_1 - k_0 C_H[O_1] \tag{10}$$

Finally, integrating Eq. (10) affords the actual value for $[O_{1d}]$, as expressed in Eq. (11)

$$\begin{aligned}[O_{1d}] = &\frac{2C_0 e^{-C_H k_0 t} k_h}{k_0^2 - 3k_0 k_h + 2k_h^2}\{-k_0[(n-2)e^{C_H(k_0-2k_h)t} - (n-1)e^{C_H(k_0-k_h)t}] \\ &+k_h[(n-2)e^{C_H(k_0-2k_h)t} - 2(n-1)e^{C_H(k_0-k_h)t} + n]\}\end{aligned} \tag{11}$$

According to Eq. (11), a general curve of the evolution of the concentration of O_{1d} (glucose) over time for the acid-catalyzed hydrolysis of cellulose in ILs can be drawn (Supplementary Fig. 2). It is clear that $[O_{1d}]$ increases over time at the early stage of the reaction, plateaus, and then decreases over time.

3.2. Fitting experimental data

The concentrations of glucose and cellobiose were monitored under typical hydrolysis conditions in ILs in the presence of different water concentrations. The reason to vary water concentrations was because water showed notable effects on cellulose hydrolysis in ILs system (Binder and Raines, 2010). Although water is the reactant, it can behave as a base to solvate the proton, and consequently, decrease the acidity of the reaction medium (Thornazeau et al., 2003). On the other hand, excess of water is also expected to reduce the glucose degradation/dehydration reactions, because these reactions are largely catalyzed by acids (Binder and Raines, 2010).

Experimental data (Supplementary Table 1) for cellobiose (scattered symbols) are shown in Fig. 1. The highest cellobiose concentrations were obtained approximately at 50, 60 and 90 min, respectively, for the reaction with water loading of 1.5, 3.0 and 4.5 mmol, which were 1.0, 2.0 and 3.0 equiv of that of AGU. It is clear that higher cellobiose concentrations were observed at a longer time point, when water contents were higher. The highest cellobiose concentrations were increased gradually with the increase of water content. These observations suggested that the rate of cellulose hydrolysis decreased because of excess water leading

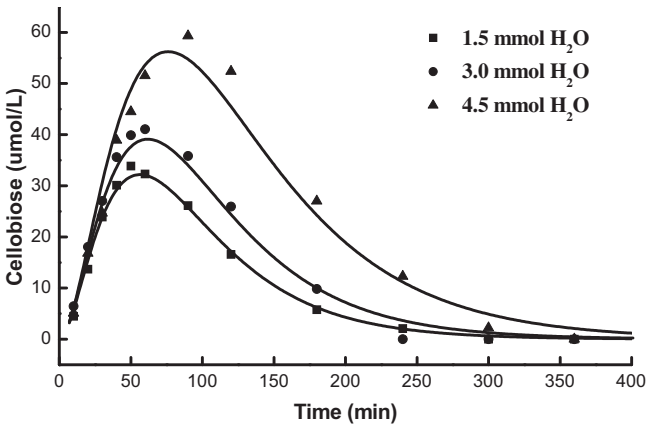

Fig. 1. Experimental data and fitting curves of cellulose hydrolysis with respect to cellobiose production. Reaction conditions: spruce cellulose 240 mg (ca. 1.5 mmol AGU), water, 4.0 g [Bmim]Cl, H_2SO_4 0.56 mmol, 94 °C.

to a reduced acidity of the reaction medium, which are in line with the "water effect" discussed above (Binder and Raines, 2010; Thornazeau et al., 2003).

To fit the experimental data, a new equation according to Eq. (9) is constructed. Because the average DP value (n) is 275 (as indicated by Sigma), and m equals to 2 for cellobiose, the function for the concentration of cellobiose can be simplified as shown in Eq. (12)

$$[O_2] = 272C_0e^{-3k_hC_Ht} - 546C_0e^{-2k_hC_Ht} + 274C_0e^{-k_hC_Ht} \quad (12)$$

Nonlinear least-squares curve fitting of experimental data according to Eq. (12) by using the MATLAB software resulted in smooth curves (Fig. 2), and the fitting parameters are listed in Table 1.

It is clear that excellent data fittings were achieved. As indicated in Eq. (12), the highest cellobiose concentration is dictated by the initial cellulose concentration (C_0). In order to give a high quality data fitting, it was necessary to vary the C_0 values when water contents were different, albeit the actual cellulose loading was identical for those reactions. While the theoretical C_0 value is estimated as 1.42 μmol mL^{-1} considering the density of [Bmim]Cl as 1.05 g mL^{-1} at 80 °C (http://www.basionics.com/en/ionic-liquids/products/data/st70.htm), the apparent C_0 values of 0.79, 0.96 and 1.38 μmol·mL^{-1}, for the reactions with water loading of 1.5, 3.0 and 4.5 mmol, respectively, were required to achieve the best data fitting. It should be pointed out that kinetic equations were constructed assuming that cellulose was dissolved and cellulose molecules were fully accessible. However, under a specified condition, a small portion of cellulose molecules may interact with each other or are not fully accessible for hydrolysis, leading to a lower apparent C_0 values. The fact that the apparent C_0 values increased concurrently with increased initial water loadings was interesting. It was suggestive that the addition of a small amount of water (up to 2.0% by weight) in ILs was actually beneficial in terms of the formation of a "real" cellulose solution.

According to Eq. (12), the parameter C_H and k_h combined together, therefore it was unable to determine the values of C_H and k_h, but only the value of $C_H * k_h$ (Table 1). Noting that k_h equals to $K_1 * k_2$, and K_1 is the equilibrium constant of the first step, i.e. the bonding between a proton and the glycosidic oxygen. When the initial water loading increased, the concentration of free proton (C_H) should be reduced due to the formation of water associated proton [H_3O^+] (Thornazeau et al., 2003). Therefore, if any changes for k_h were neglected, the value of $C_H * k_h$ was expected to decrease with the increase of initial water content, as indicated in Table 1.

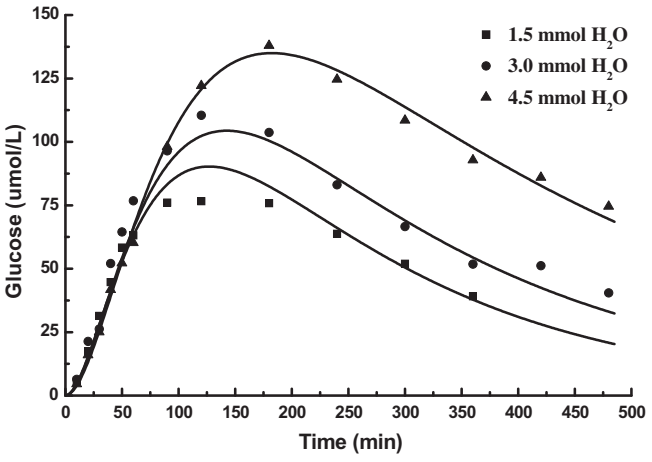

Fig. 2. Experimental data and fitting curves of cellulose hydrolysis with respect to glucose production. Reaction conditions: spruce cellulose 240 mg (1.5 mmol AGU), water, 4.0 g [Bmim]Cl, H_2SO_4 0.56 mmol, 94 °C.

Table 1
The parameter values of data fitting for cellobiose and glucose.

Entry	Water loading (mmol)	C_0 (μmol/mL)	$C_H * k_h$ (min^{-1})	k_0/k_h	Correlation coefficient[a]
1	1.5	0.79	0.0194	0.26	0.998 (0.988)
2	3.0	0.96	0.0177	0.24	0.999 (0.987)
3	4.5	1.38	0.0144	0.21	0.967 (0.997)

[a] Correlation coefficient in parentheses are associated with results of data fitting for glucose.

The experimental data for glucose (scattered symbols) are shown in Fig. 2. The highest glucose concentrations were obtained approximately at 120, 120 and 180 min for the reaction with a water loading of 1.5, 3.0 and 4.5 mmol, respectively. Similar to profiles indicated in Fig. 1, the highest glucose concentrations were observed at a longer time point when the water content was higher, and the highest glucose concentrations were increased gradually with the increase of water content.

To fit the experimental data, Eq. (11) is rewritten into Eq. (13), where $C_H * k_0$ equals to $(k_0/k_h) * (C_H * k_h)$. Therefore, Eq. (13) has two combined parameters k_0/k_h and $C_H * k_h$.

$$[O_{1d}] \equiv \frac{2C_0(n-\frac{k_0}{k_h})}{(\frac{k_0}{k_h}-1)(\frac{k_0}{k_h}-2)}e^{-C_Hk_0t} - \frac{2C_0(n-2)}{\frac{k_0}{k_h}-2}e^{-2C_Hk_ht} + \frac{2C_0(n-1)}{\frac{k_0}{k_h}-1}e^{-2C_Hk_ht} \quad (13)$$

As the values of $C_H * k_h$ and C_0 for each dataset have been established, it is straightforward to fit the glucose concentration data according to Eq. (13) and obtain values of k_0/k_h. It was found that reactive factors of 0.69, 0.65 and 0.56 were required to ensure good match for the glucose concentrations for the reactions with water loading of 1.5, 3.0 and 4.5 mmol, respectively. As shown in Fig. 2 and Table 1, data fitting by least squares techniques affords excellent results, because all fitting coefficients are close to 1.

Data fitting results showed that the values of k_0/k_h were less than one, which was consistent with early observations (Li and Zhao, 2007; Binder and Raines, 2010). The fact that k_0/k_h decreased in the presence of a higher water content suggested that the degradation reaction constant k_0 dropped. This is understandable because water consumed free proton and reduced the acidity of the solution. As a result, a higher maximum glucose concentration was achieved over a longer reaction time. The values of k_0/k_h also indicated that k_h was 4- to 5-fold higher than k_0, indicating that the hydrolysis reaction proceeded faster than the degradation reaction.

It should be emphasized that the usefulness of the current kinetic analysis is not limited to the understanding the formation of cellobiose and glucose. Because values of $C_H * k_h$ and C_0 for a given reaction condition have been available (*vide ante*), concentrations of cellooligomers of any DP values can be calculated according to Eq. (9). When the reaction was done with 3.0 mmol H_2O, concentrations of cellooligomers with DP values up to 10 can be estimated (Table 2). These data indicated that at the early stage of the reaction, cellooligomers had similar concentrations. When the reaction time elapsed, higher oligomers disappeared rapidly concurrently with the accumulation of lower oligomers. Taking [O_3] and [O_4] for example, their maximal concentrations were found at 60 min and 30 min, respectively. Albeit it remains technically challenging for quantitative analysis of cellooligomers in the hydrolysis mixture, application of the general kinetic

Table 2
Calculated concentrations of cellooligomers.

Time (min)	Concentration of cellooligomer (μmol/mL)							
	$[O_3]$	$[O_4]$	$[O_5]$	$[O_6]$	$[O_7]$	$[O_8]$	$[O_9]$	$[O_{10}]$
10	2.31	2.15	2.00	1.86	1.73	1.61	1.50	1.40
20	16.27	12.68	9.88	7.70	6.00	4.69	3.65	2.84
30	28.25	18.44	12.04	7.86	5.13	3.36	2.19	1.43
60	30.77	11.81	4.53	1.74	0.67	0.26	0.10	0.04
90	16.80	3.79	0.86	0.19	0.04	0.01	0.00	0.00
120	7.29	0.97	0.13	0.02	0.00	0.00	0.00	0.00
180	1.05	0.05	0.00	0.00	0.00	0.00	0.00	0.00
240	0.13	0.00	0.00	0.00	0.00	0.00	0.00	0.00

Reaction conditions: spruce cellulose 240 mg (AGU 1.5 mmol), H_2O 3.0 mmol, [Bmim]Cl 4.0 g, H_2SO_4 0.56 mmol, 94 °C.

equation could afford very useful information in terms of the distribution of the hydrolysis products.

4. Conclusions

In summary, general kinetic equations were formulated for acid-catalyzed cellulose hydrolysis in ionic liquids. Experimental data were fit well according to those equations, and the formation of glucose as well as cellooligomers was successfully described. Variations of kinetic parameters indicated that water behaved also as a base to decrease the acidity of the reaction medium. These results provided insights into the detailed mechanisms of homogeneous cellulose hydrolysis in a non-aqueous environment and should be valuable for developing strategies to depolymerize cellulose and lignocellulosic biomass.

Acknowledgements

Financial supports provided by the National Basic Research Program of China (2011CB707405) and the Natural Sciences Foundation of China (21002101) are greatly acknowledged.

Appendix A. Supplementary data

Supplementary data associated with this article can be found, in the online version, at doi:10.1016/j.biortech.2012.02.071.

References

Binder, J.B., Raines, R.T., 2010. Fermentable sugars by chemical hydrolysis of biomass. Proc. Natl. Acad. Sci. USA 107, 4516–4521.

Blanch, H.W., Simmons, B.A., Klein-Marcuschamer, D., 2011. Biomass deconstruction to sugars. Biotechnol. J. 6, 1086–1102.

Chheda, J.N., Huber, G.W., Dumesic, J.A., 2007. Liquid-phase catalytic processing of biomass-derived oxygenated hydrocarbons to fuels and chemicals. Angew. Chem. Int. Ed. 46, 7164–7183.

Fagan, R.D., Grethlein, H.E., Converse, A.O., Porteous, A., 1971. Kinetics of the acid hydrolysis of cellulose found in paper refuse. Environ. Sci. Technol. 5, 545–547.

Ha, S.J., Galazka, J.M., Kim, S.R., Choi, J.H., Yang, X.M., Seo, J.H., Glass, N.L., Cate, J.H.D., Jin, Y.S., 2011. Engineered *Saccharomyces cerevisiae* capable of simultaneous cellobiose and xylose fermentation. Proc. Natl. Acad. Sci. USA 108, 504–509.

Jiang, X., Gu, J., Tian, X.Z., Li, Y.L., Huang, D., 2012. Modification of cellulose for high glucose generation. Bioresour. Technol. 104, 473–479.

Kilpelainen, I., Xie, H.B., King, A., Granstrom, M., Argyropoulos, D.S., 2007. Dissolution of wood in ionic liquids. J. Agric. Food Chem. 55, 9142–9148.

Li, C.Z., Zhao, Z.K., 2007. Efficient acid-catalyzed hydrolysis of cellulose in ionic liquid. Adv. Synth. Catal. 349, 1847–1850.

Li, C.Z., Wang, Q., Zhao, Z.K., 2008. Acid in ionic liquid: an efficient system for hydrolysis of lignocellulose. Green Chem. 10, 177–182.

Nishiyama, Y., Sugiyama, J., Chanzy, H., Langan, P., 2003. Crystal structure and hydrogen bonding system in cellulose Iα from synchrotron X-ray and neutron fiber diffraction. J. Am. Chem. Soc. 125, 14300–14306.

Orozco, A.M., Al-Muhtase, A.H., Albadarin, A.B., Rooney, D., Walker, G.M., Ahmad, M.N.M., 2011. Dilute phosphoric acid-catalysed hydrolysis of municipal biowaste wood shavings using autoclave parr reactor system. Bioresour. Technol. 102, 9076–9082.

Rinaldi, R., Meine, N., vom Stein, J., Palkovits, R., Schüth, F., 2010. Which controls the depolymerization of cellulose in ionic liquids: the solid acid catalyst or cellulose? ChemSusChem 3, 266–276.

Rinaldi, R., Palkovits, R., Schüth, F., 2008. Depolymerization of cellulose using solid catalysts in ionic liquids. Angew. Chem. Int. Ed. 47, 8047–8050.

Rinaldi, R., Schüth, F., 2009. Acid hydrolysis of cellulose as the entry point into biorefinery schemes. ChemSusChem 2, 1096–1107.

Saeman, J.F., 1945. Kinetics of wood saccharification – hydrolysis of cellulose and decomposition of sugars in dilute acid at high temperature. Ind. Eng. Chem. 37, 43–52.

Sheldon, R.A., 2011. Utilisation of biomass for sustainable fuels and chemicals: molecules, methods and metrics. Catal. Today 167, 3–13.

Swatloski, R.P., Spear, S.K., Holbrey, J.D., Rogers, R.D., 2002. Dissolution of cellose with ionic liquids. J. Am. Chem. Soc. 124, 4974–4975.

Thompson, D.R., Grethlein, H.E., 1979. Design and evaluation of a plug flow reactor for acid hydrolysis of cellulose. Ind. Eng. Chem. Prod. Res. Dev. 18, 166–169.

Thornazeau, C., Olivier-Bourbigou, H., Magna, L., Luts, S., Gilbert, B., 2003. Determination of an acidic scale in room temperature ionic liquids. J. Am. Chem. Soc. 125, 5264–5265.

Vanoye, L., Fanselow, M., Holbrey, J.D., Atkins, M.P., Seddon, K.R., 2009. Kinetic model for the hydrolysis of lignocellulosic biomass in the ionic liquid, 1-ethyl-3-methyl-imidazolium chloride. Green Chem. 11, 390–396.

Vom Stein, T., Grande, P., Sibilla, F., Commandeur, U., Fischer, R., Leitner, W., de Maria, P.D., 2010. Salt-assisted organic-acid-catalyzed depolymerization of cellulose. Green Chem. 12, 1844–1849.

Zhang, Z.H., Wang, Q., Xie, H.B., Liu, W.J., Zhao, Z.K., 2011. Catalytic conversion of carbohydrates into 5-hydroxymethylfurfural by Germanium(IV) chloride in ionic liquids. ChemSusChem 4, 131–138.

Zhang, Z.H., Zhao, Z.K., 2009. Solid acid and microwave-assisted hydrolysis of cellulose in ionic liquid. Carbohydr. Res. 344, 2069–2072.